pathways. Because K is less than unity, the yield of cyclohexanone increases linearly with $Fe^{II}(DPAH)_2$ concentration. The apparent rate for the ketonization reaction is proportional to substrate concentration, $Fe^{II}(DPAH)_2$ concentration, and O_2 partial pressure and increases with temperature (about five times faster at 25 °C than at 0 °C). Because the fraction of **1** that reacts with c-C_6H_{12} remains constant (~28%), the oxidation of excess $Fe^{II}(DPAH)_2$ by **1** must be a parallel process. Given that the ratio of concentrations [c-C_6H_{12}]/[$Fe^{II}(DPAH)_2$] is about 30:1 and the ratio of reactivities is 1:2.6, the apparent relative rate constant for reaction of c-C_6H_{12} and $Fe^{II}(DPAH)_2$ with **1** is about 0.02 $k_{Fe^{II}}$ assuming a stoichiometric factor of 2 for the latter).

Addition of PhNHNHPh, H_2NNH_2, $PhCH_2SH$, or H_2S to the reaction system [O_2/Fe(DPAH)$_2$/substrate in 1.8:1 py/HOAc] reduces the oxidized catalyst [$(DPAH)_2FeOFe(DPAH)_2$] and thereby recycles it for activation of O_2 to the reactive intermediate (Table IA). When 3 mM $Fe^{II}(DPAH)_2$ is used in combination with 100 mM PhNHNHPh, the rate for the ketonization of c-C_6H_{12} is reduced by an order of magnitude, but each cycle remains about 21% efficient with 67 turnovers within 12 h.

The dioxygenation of unsaturated α-diols (catechol and benzoin, Table IB) by the $O_2/Fe^{II}(DPAH)_2$ system parallels that of the catechol dioxygenase enzymes, which are non-heme iron proteins.[6] Hence, the reactive intermediate (**1**) of the $Fe^{II}(DPAH)_2/O_2$ reaction may be a useful model and mimic for the activated complex of dioxygenase enzymes.[7]

This system affords the means to the selective autoxidation (oxygenation) of hydrocarbon substrates (e.g., c-C_6H_{12}) via the coprocessing of H_2S (or RSH)-contaminated hydrocarbon streams. Thus, the combination of c-C_6H_{12} and H_2S with $Fe^{II}(DPAH)_2$ and O_2 in 1.8:1 py/HOAc yields c-C_6H_{10}(O) and S_8 (Table IA).

Acknowledgment. This work was supported by the National Science Foundation under Grant CHE-8516247 and the Welch Foundation under Grant A-1042 with a Robert A. Welch Graduate Fellowship (C.S.).

(6) (a) Hayaishi, O.; Nozaki, M.; Abbott, M. T. In *The Enzymes*; Boyer, P. D., Ed.; Academic Press: New York, 1975, Vol. XII; pp 119-189. (b) Que, L., Jr. *Adv. Inorg. Biochem.* **1983**, *5*, 167.
(7) (a) Que, L., Jr. *J. Chem. Educ.* **1985**, *62*, 938. (b) Weller, M. G.; Weser, U. *J. Am. Chem. Soc.* **1982**, *104*, 3752.

Conformational Studies of *N*-Benzoyl-L-phenylalanine by Combined Rotation and Multiple-Pulse Spectroscopy ^1H Nuclear Magnetic Resonance

Po-Jen Chu,† Marek J. Potrzebowski,‡ Yanding Gao,‡ and A. Ian Scott*,‡

Center for Biological NMR, Department of Chemistry
Texas A&M University
College Station, Texas 77843-3255

Received August 7, 1989

A common feature encountered in amino acids, proteins, and polypeptides is the possibility of forming complex amorphous phases in the solid state through inter- and/or intramolecular hydrogen bonding, van der Waals, and electrostatic interactions.[1,2] This behavior has recently been examined by ^{13}C NMR studies of L-phenylalanine, which revealed that the dynamic and static properties of this amino acid in the solid state are influenced by the method of preparation.[3] Due to oligomerization and the formation of multicrystalline or amorphous domains, X-ray crystallographic data are only available for a few such cases. Limited by resolution and dipolar interaction of protons in solids, problems of this type have not previously been studied by observing the hydrogen bonded proton directly. Recent progress in combined rotation and multiple-pulse spectroscopy (CRAMPS) experiments has shown a dramatic improvement in sensitivity and resolution,[4] and in some diamagnetic solids, a proton resolution as high as ~0.2 ppm has been achieved.[5,6] Previously, the relationship between the inter-oxygen distance $R_{O\cdots O}$ and proton chemical shift of -O-H···O= type H bonding was established by using the homonuclear proton-proton dipolar decoupling technique[7] of a series of carboxylic acid single crystals. The correlation was later repeated and improved for carboxylic acid polycrystalline samples with use of the CRAMPS technique.[6] Recently we have also obtained an empirical correlation, $R_{O\cdots O}$ (Å) = 2.97 - 0.0276δ (ppm), from a series of amino acids and carboxylic acids for nearly linear -O-H···O=C bonds.[8] This relation is found to be valid also for polyaminopolycarboxylic acids such as DTPA, EGTA, and EDTA where the H-bonding network is more complicated.[8] We now show that ^1H CRAMPS experiments and the shift-distance correlation can be used to deduce the geometric parameters and possible conformations for various hydrogen bonded arrays of solid samples of *N*-benzoyl-L-phenylalanine (*N*-Bz-Phe).

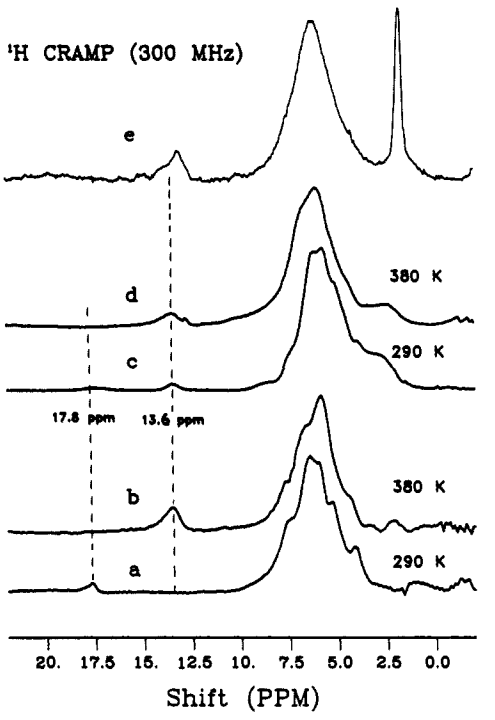

Figure 1. Proton CRAMPS spectra for *N*-benzoyl-L-phenylalanine for sample A (a, b), sample B (c, d), and sample C (e). Traces b and d correspond to the results after heating the samples to 380 °K. The sharp peak at 1.76 ppm in spectrum e is the adamatane internal reference.

Three samples of *N*-Bz-Phe were prepared by different methods. Sample A was crystallized from chloroform or triturated with hexane:ethyl acetate from acetone solution. Sample B was crystallized from water:ethanol, water:acetone, or hot water solution with slow cooling, and sample C was crystallized from hot water followed by rapid cooling to room temperature.[9] Shown

† Department of Chemistry.
‡ Center for Biological NMR.
(1) Opella, S. J. *Annu. Rev. Phys. Chem.* **1982**, *33*, 533.
(2) Smith, S. O.; Griffin, R. G. *Annu. Rev. Phys. Chem.* **1988**, *39*, 511.
(3) (a) Frey, M. H.; DiVerdi, J. A.; Opella, S. J. *J. Am. Chem. Soc.* **1985**, *107*, 7311. (b) Schaffer, J.; Stejskal, E. O.; McKay, R. A.; Dixon, W. T. *J. Magn. Reson.* **1984**, *57*, 85.
(4) (a) Gerstein, B. C. *Phil. Trans. Roy. Soc. London* **1981**, *A299*, 521. (b) Gerstein, B. C.; Pembelton, R. G.; Wilson, R. C.; Ryan, L. M. *J. Chem. Phys.* **1977**, *66*, 361. (c) Gerstein, B. C.; Dybowski, C. In *Transient Techniques in Solid State NMR*; Academic Press: New York, 1985.
(5) Bronnimann, C. E.; Hawkins, B. L.; Zhang, M.; Maciel, G. E. *Anal. Chem.* **1988**, *60*, 1743.
(6) Harris, R. K.; Jackson, P. L.; Merwin, H.; Day, B. J.; Hägde, G. *J. Chem. Soc., Faraday Trans. 1* **1988**, *84*, 3649.
(7) (a) Berglund, B.; Carson, D. G.; Vaughan, R. W. *J. Chem. Phys.* **1980**, *72*, 824. (b) Berglund, B.; Vaughan, R. W. *J. Chem. Phys.* **1980**, *73*, 2037.
(8) Chu, P. J.; Reibenspies, J. Submitted for publication.

0002-7863/90/1512-881$02.50/0

in Figure 1 are the CRAMPS spectra for the three specimens.[10] Resonances between 6.0 and 8.0 ppm correspond to the aromatic protons. The aliphatic protons of the α and β carbons resonate between 1 and 4 ppm and the N–H···O= type protons are located between 2 and 10 ppm. These values do not differ appreciably from that of the corresponding protons in solution phase. The most interesting features are the resonances between 10 and 20 ppm that are attributed to the protons in the O=C–O–H···O= carboxylic hydrogen bonds. As the H-bond strength increases, proton electron density becomes more equally shared between two oxygens, resulting in the shortening of the O···O distance and a downfield shift (deshielding) of the proton resonance. Because these resonances are far removed from those of other functional groups, the chemical shifts of the various hydrogen bonded species can be precisely identified. For the triturated sample, A, a single resonance at 17.8 ppm at room temperature (Figure 1a) is observed, which is displaced to 13.6 ppm after the sample is heated to 380 K (Figure 1b). The room temperature CRAMPS spectrum for sample B (Figure 1c) shows two resonances at 13.6 and 17.8 ppm. After this sample was gradually heated to 380 K, the intensity of the resonance at 17.8 ppm species diminishes while that at 13.6 ppm increases (Figure 1d). Sample C displayed an identical resonance at 13.6 ppm both before and after the heat treatment (Figure 1e).[11] From the linear correlation obtained previously, the $R_{O\text{-}O}$ distances in the H bonding in the different *N*-Bz-Phe samples are estimated to be 2.48 Å (17.8 ppm) and 2.59 Å (13.6 ppm), respectively. These results agree well with those obtained from ref 6 and clearly suggest the existence of at least two independent conformations with different H-bond distances in the lattice formed through the –O–H···O= type hydrogen bond during the oligomerization of *N*-Bz-Phe. Due to the difference of the thermal stability of the individual conformations, different structures result from each method of preparation.

In confirmation of the applicability of this shift–distance correlation the proton CRAMPS spectrum of *tert*-butoxycarbonyl-L-phenylalanine showed a single peak at 13.4 ppm, a broad aromatic peak below 8 ppm, and an aliphatic (*t*-Bu) peak below 4 ppm. From the single resonance at 13.4 ppm, a $R_{O\text{-}O}$ distance of 2.60 Å is predicted. From single-crystal studies the donor–acceptor distance ($R_{O\text{-}O}$ and $R_{N\text{-}O}$) in the two types of H bonds equals 2.61 Å in the –O–H···O= type H bond and 2.99 Å in the >N–H···O= type H bond, respectively.[12] Thus the O···O distances obtained from X-ray and NMR measurements are fully consistent. As mentioned previously, signals for protons in >N–H···O= H bonds are much broader with isotropic shift ranges between 2 and 10 ppm, which overlap with the aromatic and aliphatic resonances and cannot be unambiguously assigned. However, the latter bonding can be studied by ^{13}C NMR since the carbonyl ^{13}C chemical shift and the $R_{N\text{-}O}$ distance in >N–H···O=C type hydrogen bond can be correlated.[13] This type of H bonding may be better studied through ^{13}C NMR and not by ^{1}H CRAMPS.

Among all possible conformations, only two forms are thermodynamically plausible and show a –O–H···O= type hydrogen bonding with $R_{O\text{-}O}$ distance close to that predicted from the proton shift. These two structures are shown in Figure 2. Form I shows that *N*-Bz-Phe molecules fused symmetrically by two H bonds of either –O–H···O= type or >N–H···O= type, while form II displays the *N*-Bz-Phe molecules fused asymmetrically by the two types of H bonds with the same H-bond configuration repeated between molecules. Two distinct –O–H···O= type H bonds are present with O···O distances equal to 2.50 Å (I) and 2.60 Å (II), respectively. The N···O distances in the >N–H···O= type H bond were derived from ^{13}C carbonyl chemical shifts as described elsewhere.[14] From molecular mechanics calculations,[15] is is also found that structure II possesses the lowest repulsive energy and is considered to be the most thermodynamically stable configuration. On the basis of these considerations and the variation of the H-bonded proton shift with heating, we conclude that almost all of sample A and part of sample B is initially composed of structure I bridging through two symmetric (and stronger) O–H···O= H bonds. After heating samples A and B to 380 K, this phase undergoes an irreversible rearrangement to the most thermodynamically favored conformation (form II), where the weaker H bond gives rise to a proton resonance at 13.6 ppm. Notice that the two conformations shown here can be readily exchanged by rotating the central N-Bz-Phe by 180°. These results do not exclude the existence of minor contributions from other conformations with different phenyl ring and α carbon orientations, but the basic framework structure should be similar to those described here.[16]

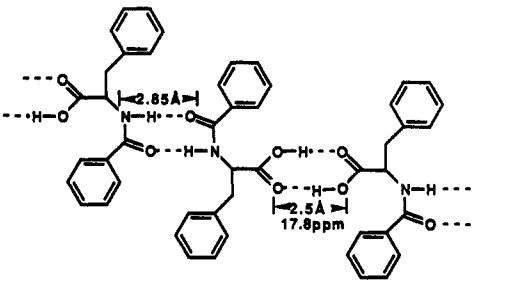

I

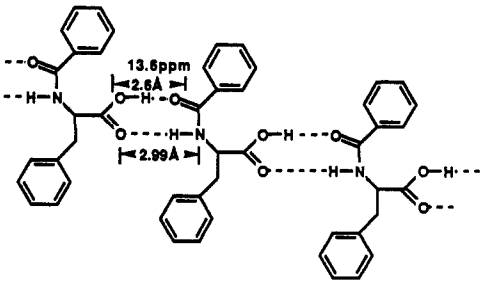

II

Figure 2. Two plausible structures for *N*-benzoyl-L-phenylalanine with the shift values and calculated O···O distances from molecular mechanics calculation.

In summary, the current study demonstrates that, in the absence of crystallographic parameters or other structural information, the O···O bond distance in hydrogen-bonded structures can be inferred from high-resolution solid-state proton NMR and hence thermodynamically plausible structures can be inferred for peptides and amino acids in the solid state. Although precise atomic positions and the unit lattice parameters can be determined only

(9) *N*-Bz-phe is a commercial sample from Sigma. CRAMPS spectra are identical for alternative preparations of samples A&B.

(10) Proton CRAMPS experiments were performed on a Bruker MSL-300 spectrometer equipped with a Bruker probe. BR-24 pulse sequence, with 1 μs proton 90° pulse, sample spinning rate between 1.5 and 2 kHz and 5 s repetition delay. Tuning of the pulse phases and the pulse width were performed according to the scheme described in ref 4a. Precautions are taken with the non-constant scaling factors associated with the multiple-pulse experiment, which can introduce a large error in H-bond proton resonances if not corrected. Spinning side bands and spurious rotor frequencies were identified and removed by varying proton offset and spinning frequency. Adamantane (δ = 1.76 ppm, line width ~0.3 ppm) was used as an internal standard for accurate chemical shift measurement.

(11) The acid proton at 17.8 ppm has a longer T_1 relaxation time. When recycle delay increases to 20 s the areas between 17.8 and 13.6 ppm become nearly equal in Figure 1a.

(12) Bats, J. W.; Fuess, H.; Kessler, H.; Schuck, R. *Chem. Ber.* **1980**, *113*, 520.

(13) (a) Ando, S.; Yamanabe, T.; Ando, I.; Shoji, A.; Ozaki, T.; Taheta, R.; Saito, H. *J. Am. Chem. Soc.* **1988**, *110*, 7648. (b) Ando, S.; Ando, I.; Shoji, A.; Ozaki, T. *J. Am. Chem. Soc.* **1988**, *110*, 3380.

(14) Potrzebowski, M. J.; Chu, P.-J.; and Scott, A. I. Manuscript in preparation.

(15) Molecular mechanics calculation was performed according to the algorithm described in: Burkert, U.; Allinger, N. L. In *Molecular Mechanics*; ACS Monograph 177; Caserio, M. C., Eds.; American Chemical Society: Washington, DC 1982.

(16) The observed shift changes are not due to dehydration since the sample is not hygroscopic; the chemical shift change is discreet and sudden before and after heat treatment and the CRAMPS spectra do not vary when samples were exposed to air for an extended period.

by crystallography, the current method leads to the derivation of molecular structures and interactions between molecules in systems where a single-crystal study is not available. To the best of our knowledge, the example presented here is the first ^1H CRAMPS NMR study concerning the thermal phase alteration of amino acids in the solid state.

Acknowledgment. We thank the National Institutes of Health and the Robert A. Welch Foundation for financial support of this work. We also thank Dr. B. C. Gerstein (Ames) and Robert Taylor (Bruker) for helpful discussions concerning the CRAMPS experiments.

Phthalimide Hydroperoxides as Efficient Photochemical Hydroxyl Radical Generators. A Novel DNA-Cleaving Agent

Isao Saito,* Masami Takayama, and Teruo Matsuura

Department of Synthetic Chemistry
Faculty of Engineering, Kyoto University
Kyoto 606, Japan

Seiichi Matsugo

Kobe University of Mercantile Marine
Fukae-minami 5-1, Kobe 658, Japan

Shosuke Kawanishi

Department of Public Health, Faculty of Medicine
Kyoto University, Kyoto 606, Japan

Received October 6, 1989

While a variety of methods for the generation of hydroxyl radical are known,[1] the use of organic hydroperoxides as a hydroxyl radical source has not been fully realized.[2,3] Hydroperoxides that can efficiently generate hydroxyl radical by photoirradiation with long-wavelength light (>300 nm) without using metal ions would be an extremely useful hydroxyl radical source, particularly for the design of DNA-cleaving molecules.[3] We report herein an efficient method for generating hydroxyl radical by irradiation (>300 nm) of hydroperoxides derived from phthalimides, which may be widely used as a convenient and clean hydroxyl radical source. We also disclose their use as an effective photochemical DNA cleaver.

Our strategy for generating hydroxyl radical is based on the photochemical γ-hydrogen abstraction of phthalimide[6] and the earlier finding[7] that the hydroperoxyalkyl radicals such as **1** undergo extremely facile β-cleavage of the labile O–O bond giving rise to hydroxyl radical as illustrated in Scheme I. Since γ-hydroperoxy ketones normally exist in a cyclic peroxide form, we have chosen hydroperoxides derived from phthalimides as the precursor. Hydroperoxides **2** and **3** are readily available by singlet oxygenation of **4** in a 1:1 ratio, whereas **5** and **6** were prepared from the corresponding dimethyl ketals (ethereal H_2O_2/cat. CF_3SO_3H/0 °C, 80–85%).[8] Hydroperoxide **7** was obtained from

Scheme I

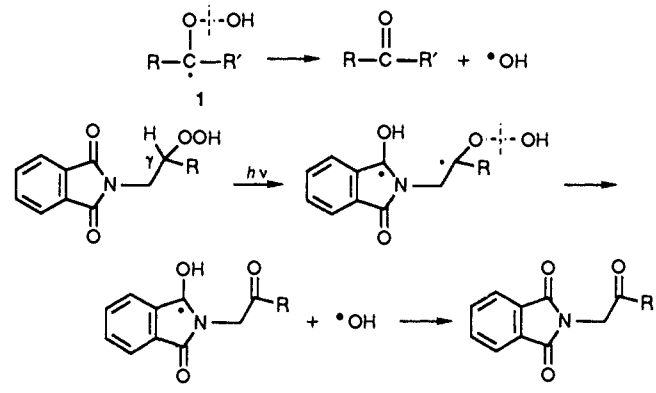

8 (H_2O_2/CF_3SO_3Ag/ether/0 °C, 70%), whereas **9** was prepared by singlet oxygenation of **10** together with an isomeric hydroperoxide. These hydroperoxides purified by silica gel column chromatography were stable in aqueous organic solvents for at least 10 h at ambient temperature.

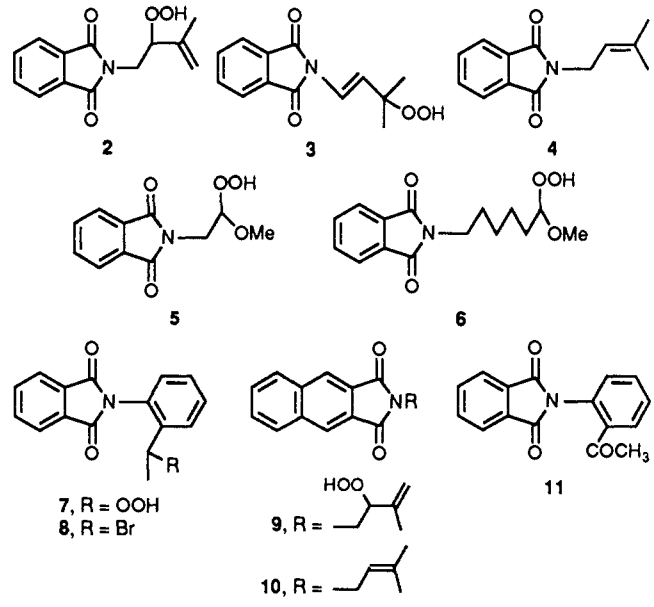

Upon photoexcitation, phthalimide derivatives **2** and **5** possessing a secondary hydroperoxy group at the γ-position induce hydroxylation of saturated hydrocarbons and benzene. For example, external irradiation of a solution of **2** (32 mM) in benzene in a sealed test tube with a 100-W high-pressure mercury lamp through a Pyrex filter (>280 nm) for 7 h at ambient temperature produced phenol (10%),[9] whereas irradiation of a solution of **2** (2 mM) and adamantane (10 mM) in acetonitrile under aerobic conditions for 2 h followed by extractive workup with *n*-pentane provided 1-adamantanol (25%), 2-adamantanol (7%), and adamantanone (7%).[9,10] Preferential attack on the tertiary

(1) (a) Czapski, G. *Methods Enzymol.* **1984**, *105*, 209. (b) Walling, C. *Acc. Chem. Res.* **1975**, *8*, 125. (c) Bielski, B. H.; Gebicki, J. M. *Free Radicals Biol.* **1977**, *3*, 1. (d) Halliwell, B.; Gutteridge, M. C. *Biochem. J.* **1984**, *219*, 1. (e) Sie, H. *Oxidative Stress*; Academic Press: New York, 1985.

(2) Ogata, Y.; Tomizawa, K.; Furuta, K. *The Chemistry of Peroxides*; Patai, S., Ed.; Wiley: New York, 1983; p 711.

(3) While the generation of hydroxyl radical by 254-nm irradiation of hydrogen peroxide and alkyl hydroperoxides has been well established,[2] only few are known for the unimolecular photochemical generation of hydroxyl radical by irradiation of hydroperoxides with long-wavelength light. These examples include photochemical generation of hydroxyl radical from α-keto hydroperoxides[4] and α-azo hydroperoxides.[5]

(4) Sawaki, Y.; Ogata, Y. *J. Am. Chem. Soc.* **1976**, *98*, 7342.

(5) Tezuka, T.; Narita, N. *J. Am. Chem. Soc.* **1979**, *101*, 7413.

(6) (a) Coyle, J. D. *Synthetic Organic Photochemistry*; Horspool, W. H., Ed.; Plenum: New York, 1984. (b) Mazzocchi, P. H. *Org. Photochem.* **1981**, *5*, 421. (c) Kanaoka, Y. *Acc. Chem. Res.* **1978**, *11*, 407.

(7) (a) Russell, G. A. *Free Radicals*; Kochi, J. K., Ed.; Wiley: New York, 1973. (b) Howard, J. A.; Chenier, J. H. B. *Can. J. Chem.* **1980**, *58*, 2808.

(8) Myers, A. G.; Fundy, M. M.; Lindstrom, P. A., Jr. *Tetrahedron Lett.* **1988**, *29*, 5609.

(9) Yields determined by GC are based on hydroperoxides initially used.

(10) Products derived from **2** were *N*-(2-methyl-3-oxo-1-buten-4-yl)-phthalimide (10%), *N*-(hydroxymethyl)phthalimide (i) (68%), and methacrolein (ii) (64%) under aerobic conditions. While the former product results from γ-hydrogen abstraction (Scheme I), the latter two products (i and ii) are assumed to arise from β-scission of radical iii formed via homolysis of hydroperoxide **2** initiated by intramolecular energy transfer from photoexcited phthalimide chromophore. Mechanistic details of the photoreaction of these hydroperoxides will be published in a forthcoming paper.

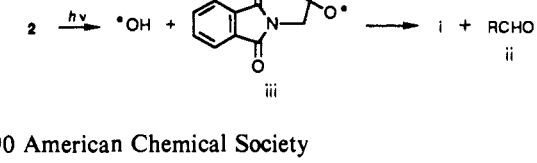

0002-7863/90/1512-883$02.50/0